ELSEVIER

Applied Surface Science 166 (2000) 179–184

applied surface science

www.elsevier.nl/locate/apsusc

(001) Surfaces of GaP and InP: structural motifs, electronic states and optical signatures

W.G. Schmidt [a,*], J. Bernholc [a], F. Bechstedt [b]

[a] *Department of Physics, North Carolina State University, Raleigh, NC 27695-8202, USA*

[b] *Institut für Festkörpertheorie und Theoretische Optik, Friedrich-Schiller-Universität, Max-Wien-Platz 1, 07743 Jena, Germany*

Abstract

We present ab initio calculations on the energetics and geometry, as well as electronic and optical properties of InP and GaP(001) surfaces. Cation-rich conditions lead to the formation of asymmetric cation–anion dimers on top of a (2×4) reconstructed cation-terminated surface. Anion-rich surfaces form $c(4\times4)$ reconstructions. Based on the DFT-LDA electronic structure, we compute the reflectance anisotropy of the energetically favoured (2×4) reconstructions. Strong anisotropies in the low-energy region arise from transitions between σ-like cation–cation bonding states and empty dangling bonds. Transitions involving P dimer states and surface modified bulk wave functions contribute at higher energies. The application of *GW* corrections leads to non-uniform shifts of characteristic peaks and changes the line shape, considerably improving the agreement with experiment. © 2000 Elsevier Science B.V. All rights reserved.

PACS: 78.30.Fs; 68.35.Bs; 71.15.Mb; 71.10.-w

Keywords: Gallium phosphide; Indium phosphide; (001) Surfaces; Reflection spectroscopy; Density functional calculations; Excitation spectra calculations

1. Introduction

There is strong scientific interest in III–V(001) surfaces, arising from the abundant, highly coverage-dependent surface structures. In particular, there are many open questions concerning GaP and InP [1,2]. Only recently, it was shown that cation-rich GaP and InP surfaces form (2×4) reconstructions [3,4]. The P-rich surface structures are essentially unknown [5,6]. The InP(001) surface electronic structure has been subject to both experimental [7,8] and theoretical investigations [9], but no studies are available for GaP. Both GaP [3,10,11] and InP [12–14] surfaces, however, have been thoroughly studied by reflectance anisotropy spectroscopy (RAS). The present work aims at a comprehensive picture of the stoichiometry-dependent atomic structures of GaP and InP(001) surfaces and their electronic and optical properties.

2. Method

We perform first-principles density-functional (DFT-LDA) calculations using nonlocal pseudopotentials and a real-space multigrid technique [15]. The electronic wave functions are mapped on a grid

* Corresponding author. Permanent address: Institut für Festkörpertheorie und Theoretische Optik, Friedrich-Schiller-Universität, Max-Wien-Platz 1, 07743 Jena, Germany. Tel.: +49-3461-635910; fax: +49-6341-635182.

E-mail address: w.g.schmidt@ifto.physik.uni-jena.de (W.G. Schmidt).

0169-4332/00/$ - see front matter © 2000 Elsevier Science B.V. All rights reserved.
PII: S0169-4332(00)00406-2

with a spacing of 0.24 Å. Periodic super cells containing eight (12) atomic (001) layers and a vacuum region eight atomic layers thick are used to calculate the energetic (optical) surface properties. Integrations in the surface Brillouin zone for calculating the atomic and electronic ground state were performed using four special k points in the irreducible part. For the calculation of the dielectric function in the independent-particle approximation, we include all conduction bands within 8 eV of the top of the valence band, using 16 uniformly distributed k points in the irreducible part. Further details are given in Ref. [16].

The calculation of optical properties within DFT-LDA neglects the quasiparticle character of electrons. In order to study the influence of these many-body effects, we go in one instance beyond the DFT-LDA. In the quasiparticle picture of electronic excitations, the nonlocal and energy-dependent self-energy operator $\Sigma(r, r'; E)$ replaces the local exchange and correlation potential used in the DFT-LDA. However, even in its lowest so-called *GW* approximation, where Σ is expressed as the product of the single-article propagator G with the dynamically screened Coulomb interaction W, its calculation remains a formidable task, in particular, for the large number of states entering the surface dielectric function. Therefore, we had to introduce further approximations. Following Bechstedt et al. [17], we use a model dielectric function where local-field effects are approximately included via its density dependence. A single plasmon-pole approximation is employed to account for the dynamical effects. The model requires the input of the dielectric constant ε_∞, and its application to surfaces therefore seems problematic. However, Northrup [18] and Rohlfing et al. [19] have shown that the final band structure does not depend very much on the actual value of ε_∞ and that such models can justifiably be used for surface *GW* calculations.

3. Results

3.1. Surface energies and structures

To determine the ground state geometries for GaP and InP(001), we investigated a large number of plausible surface structures. For cation-rich surfaces, we started with the models discussed in Ref. [4], but included further structures, notably the (2×4) geometry, which is assumed to describe the Sb-induced (2×4) reconstruction of GaAs [20]. For anion-rich surfaces, we studied three c(4×4) geometries: The two- and three-dimer geometries discussed for GaAs [21,22], as well as a three-P-layer model recently suggested by Ozanyan et al. [6]. In order to compare the structures energetically, one has to take into account the chemical potentials μ of the surface constituents [23]. The resulting phase diagrams, containing only the energetically favoured GaP and InP surface structures, are shown in Fig. 1. A top view of the GaP surface models is given in Fig. 2. The corresponding InP surface geometries are very similar.

Cation-rich GaP and InP surfaces are characterized by a sequence of (2×4) single-dimer reconstructions. This is in stark contrast to cation-rich GaAs(001) surfaces, where sp^2-hybridized Ga dimers form (4×2) reconstructions [23]. A possible explanation for this difference is the larger relative size of the cations in case of the phosphide surfaces. It hinders the accommodation of dimers formed by sp^2-hybridized cations. The formation of mixed-dimer and top-Ga-dimer structures, as predicted here, agrees with a recent general study on the stability of semiconductor surfaces [24]. Mixed-dimer geometries give a natural explanation for the surface core-

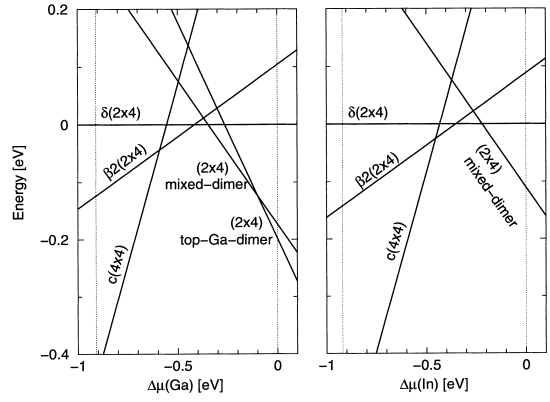

Fig. 1. Relative formation energy per (1×1) unit cell for GaP (left panel) and InP (right panel) surface reconstructions vs. the respective cation chemical potential. Dashed lines mark the thermodynamically allowed range between the extreme anion- and cation-rich conditions.

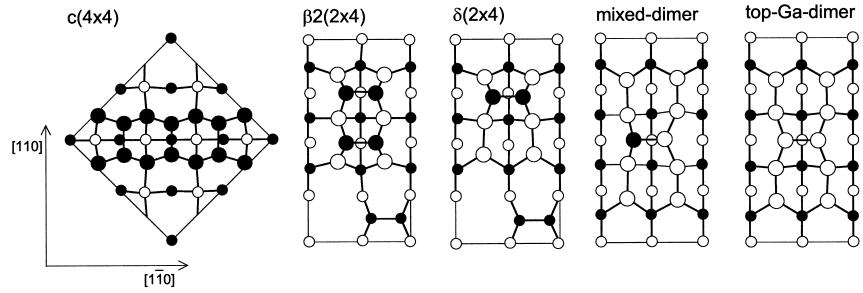

Fig. 2. Top view of GaP(001) surface reconstruction models. Empty (filled) circles represent Ga (P) atoms. Large (small) symbols indicate positions in the first and second (third and fourth) atomic layers.

level shifts measured on cation-rich GaP [25] and InP surfaces [4] and may explain the characteristic asymmetry observed by STM [2]. The observation of a surface P component in the photoemission spectrum of the Ga-rich GaP surface indicates that the extreme Ga-rich limit, which should be characterized by the formation of single Ga dimers according to our calculations, may actually not be reached in the experiments. For more anion-rich surfaces $\beta 2(2\times 4)$ and $c(4\times 4)$ reconstructions form, featuring anion dimers as known from GaAs. The calculated surface phase diagram is in agreement with the existing experimental findings for InP [12] stating (2×4) and $c(4\times 4)$ surface reconstructions for cation- and anion-rich surfaces. It does not explain, however, the intermediate $(2\times 1)/(2\times 2)$ surface phase [5]. None of the investigated $(2\times 1)/(2\times 2)$ reconstructions in our study was energetically stable.

3.2. Electronic properties

We focus here on the electronic structure of the mixed-dimer model of GaP(001), which has been identified as the most likely geometry for the Ga-rich (2×4) surface [3]. It is also the most interesting from a surface science point of view, as the elec-

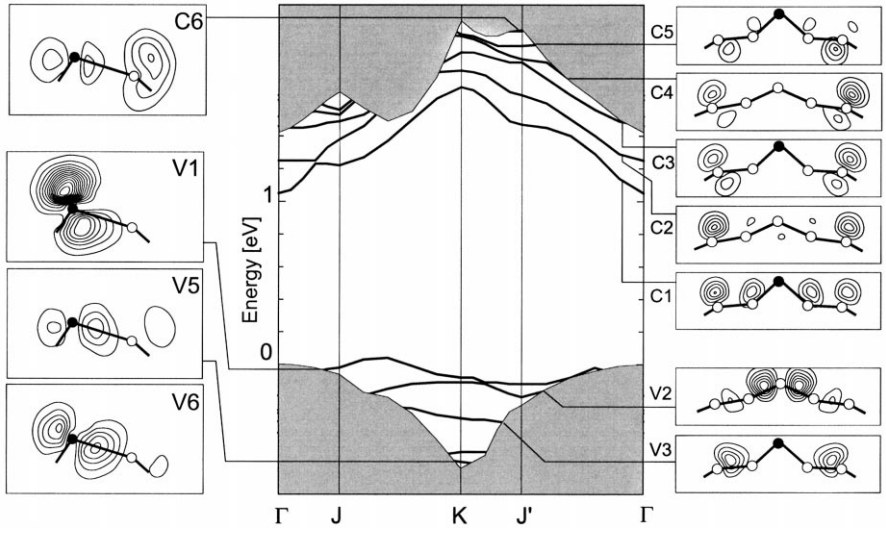

Fig. 3. Surface band structure (bound states) for the mixed-dimer structure of GaP(001). Gray regions indicate the projected bulk band structure. In the left and right panel, the corresponding squared wave functions at K are shown. The contour spacing is 10^{-3} bohr^{-3}.

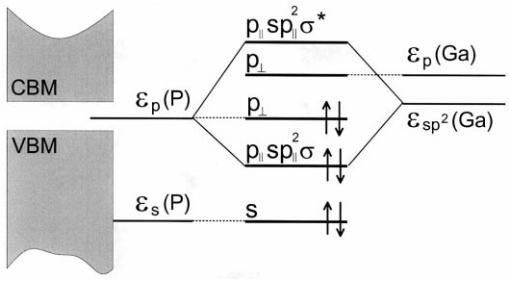

Fig. 4. Schematic energy level diagram for the mixed-dimer localized states at the Ga-rich GaP(100)(2×4) surface.

tronic states associated with symmetric dimers have been analysed previously [20,23,26]. Results for InP are given in Ref. [9]. In Fig. 3, the surface bands of the mixed-dimer model together with their orbital character are shown. The highest occupied surface state, V1, slightly above the bulk valence band edge, corresponds to the P dangling bond at the mixed dimer. The σ-bonding dimer states V5 and V6, 0.5 and 0.7 eV below the bulk valence-band maximum (VBM) at the K point, are mainly degenerate with bulk bands. The corresponding anti-bonding combinations lie above the bulk band gap. C6, derived from the empty Ga *p* orbital at the mixed dimer, is a bound surface state only for a small region around J'. In the upper part of the bulk band gap lie also several unoccupied surface bands, C1–C5, which arise from dangling bonds at the second-layer surface cations. V2 and V3, slightly below the VBM, are related to σ-like bonds between surface Ga atoms.

The bonding of the mixed dimer is different from the usual cation–cation or anion–anion dimers at III–V(001) surfaces. Cation dimers are characterized by single σ bonds formed by sp^2 hybrids [23], whereas for anion dimers, the σ, π and π^* combinations of the anion *p* orbitals are occupied [26]. For the hybrid GaP dimer, the in-plane anion *p* and cation sp^2 orbitals form a σ bond (cf. Fig. 4). A very similar picture holds for the mixed dimers formed at InP(001) [8,9].

3.3. Optical properties

In Fig. 5, we show the reflectance anisotropy spectra calculated for the energetically favoured (2×4) surface reconstructions of InP and GaP. The top-Ga-dimer and mixed-dimer structures show a pronounced negative anisotropy in the low energy region, with minima at 1.7 eV for InP(001) and 2.0–2.3 eV for GaP(001). That anisotropy is correlated to surface cation–cation bonds along [110]: Its magnitude is highest for the top-Ga-dimer model

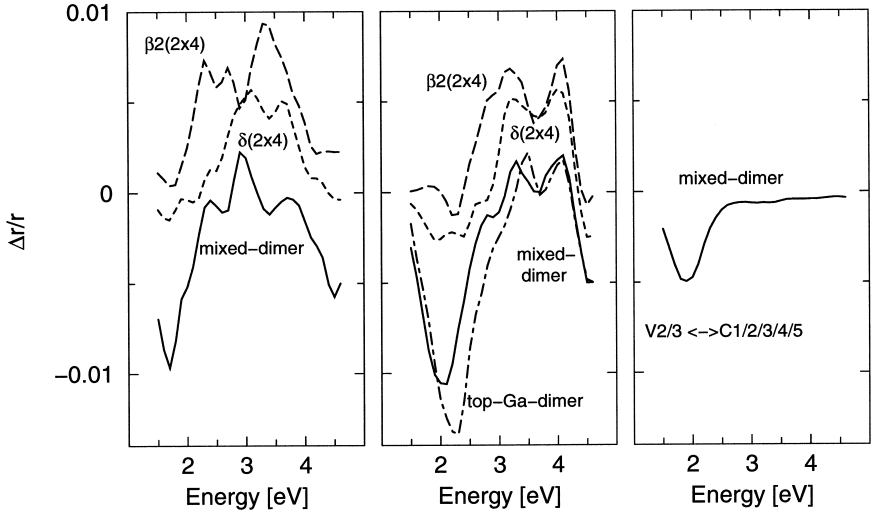

Fig. 5. RA spectra $[Re\{(r_{[1\bar{1}0]} - r_{[110]})/\langle r \rangle\}]$ calculated for InP (left panel) and GaP(001) (2×4) surface structures (middle). In the right panel, we show the RA of the GaP (001) mixed-dimer model from transitions between surface states V2/V3 and C1–C5 (cf. Fig. 3) only.

with eight bonds, somewhat reduced for the mixed-dimer geometry with six cation–cation bonds and much flattened for the δ structure with only two such bonds. The calculated spectra also show a strong dependence on structural details for higher energies. For the $\beta 2$ geometry with three P dimers oriented along $[1\bar{1}0]$, we find a relatively broad positive anisotropy between 2 and 4 eV for InP and between 2.4 and 4.4 eV for GaP. This positive anisotropy is somewhat reduced for the δ structure, with only two P dimers. The appearance of strongly stoichiometry-dependent, signature-like features in the RA spectra closely parallels the evolution of the experimental spectra measured for different surface preparation conditions [3,12].

In order to understand the origin of these fingerprints, we performed further calculations and separated the contribution of the transitions between the cation-derived, bound surface states V2/V3 and C1–C5 (cf. Fig. 3) to the reflectance anisotropy of the mixed-dimer structure of GaP. The result is shown in the right panel of Fig. 5. The transitions involving exclusively these seven surface states account, to a large extent, for the negative anisotropy associated with the existence of surface cation–cation bonds. Earlier, we have shown that transitions between surface resonances and P-dimer-related states are largely responsible for positive anisotropies at higher energies [16].

However, not all features observed in the spectra depend on the surface structure and chemistry: For example, all spectra calculated for GaP(001)(2×4) have a maximum slightly above 4 eV, the calculated energy of the E_0' critical point. Calculations that spatially separate the contributions to the RA from transitions within the surface layers and the layers underneath show that this maximum is indeed due to transitions between surface modified bulk states. Similar bulk band structure related features are observed in the surface RA of InP(001) [16,27].

Although the qualitative agreement between the DFT-LDA calculations and measured spectra is good, in particular with respect to the chemical trend, the quantitative description in unsatisfactory. This is demonstrated in Fig. 6, where the DFT-LDA spectrum for the mixed-dimer model of GaP is compared with the corresponding experiment [3]. The main problem concerns the peak positions: The E_0' related

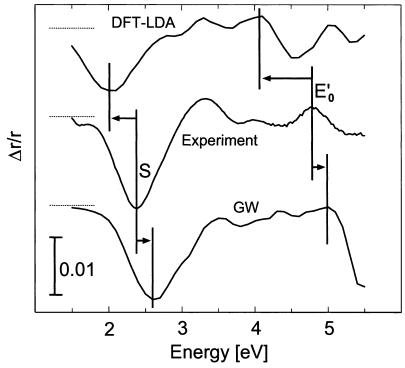

Fig. 6. RA spectra calculated for the mixed-dimer model of the GaP(001) surface within DFT-LDA and GW compared to the corresponding experiment [3]. Surface and bulk-related features *S* and E_0' are indicated.

maximum is measured at an energy of about 4.8 eV. In the calculations, it occurs at 4.1 eV. A somewhat smaller underestimation occurs for the surface related feature *S*. These underestimations are caused by the DFT-LDA band gap problem. To account for that, we correct the spectrum using the *GW* approach described in Section 2. The main effect is a non-uniform shift of the excitation energies to higher values. In agreement with the experiment, we observe a stronger shift for the bulk related features compared to the surface states. In addition to these shifts, the line shape of the spectrum also changes: The weak shoulder at 2.8 eV in the DFT-LDA spectrum develops into a maximum at 3.5 eV, in good agreement with experiment. While the agreement between the measured and the calculated spectra improves much upon inclusion of *GW* corrections, there remain discrepancies: The excitation energies are somewhat overestimated and the line shapes, in particular, for higher energies, do not agree very well. This is partially due to the increased energy splitting caused by the underestimation of the experimental lattice constant by 1.1% in our calculation, but probably also an artifact of the approximate treatment of local-field effects in our *GW* approach and the neglect of electron–hole interactions [28]. Furthermore, the measurements were made at 300 K, whereas the calculation does not include temperature effects, which lead to a redshift of the optical spectrum by about 0.1 eV [29].

4. Summary

We presented ab initio calculations on GaP and InP(001) surfaces. Depending on the preparation conditions, we predict similar sequences of (2×4) structures for cation-rich and the formation of c(4×4) reconstructions for anion-rich GaP and InP surfaces. For cation-rich surfaces, σ-bonded, hybrid III-P dimers on top of a cation-terminated substrate are formed. The calculated RA spectra show characteristic "signatures" from surface states, as well as derivative-like features caused by surface modified bulk wave functions. DFT-LDA gives a reasonable qualitative description of the experimental spectra. Many-body corrections in *GW* approximation lead, however, to a substantial improvement.

Acknowledgements

We acknowledge support by the DFG (Schm 1361/1-1), the NSF (DMR 9408437) and the ONR (N00014-96-I-0161), as well as grants of computer time from the DoD Challenge Program and the North Carolina Supercomputer Center.

References

[1] Q.K. Xue, T. Hashizume, T. Sakurai, Prog. Surf. Sci. 56 (1997) 1.
[2] C.D. MacPherson, R.A. Wolkow, C.E.J. Mitchell, A.B. McLean, Phys. Rev. Lett. 77 (1996) 691.
[3] A.M. Frisch, W.G. Schmidt, J. Bernholc, M. Pristovsek, N. Esser, W. Richter, Phys. Rev. B 60 (1999) 2488.
[4] W.G. Schmidt, F. Bechstedt, N. Esser, M. Pristovsek, C. Schultz, W. Richter, Phys. Rev. B 57 (1998) 14596.
[5] L. Li, B.-K. Han, Q. Fu, R.F. Hicks, Phys. Rev. Lett. 82 (1999) 1879.
[6] K.B. Ozanyan, P.J. Parbrook, M. Hopkinson, C.R. Whitehouse, Proceedings of the 24th Int. Conf. on the Physics of Semiconductors, World Scientific, Singapore, 1998.
[7] W.R.A. Huff, M. Shimomura, N. Sanada, G. Kaneda, T. Takeuchi, Y. Suzuki, H.W. Yeom, T. Abukawa, S. Kono, Y. Fukuda, Phys. Rev. B 57 (1998) 10132.
[8] A.M. Frisch, P. Vogt, S. Visbeck, T. Hannappel, F. Willig, W. Braun, W. Richter, J. Bernholc, W.G. Schmidt, N. Esser, Appl. Surf. Sci. 166 (2000) 224.
[9] W.G. Schmidt, F. Bechstedt, Surf. Sci. 409 (1998) 474.
[10] P.A. Postigo, G. Armelles, T. Utzmeier, F. Briones, Phys. Rev. B 57 (1998) 1359.
[11] M. Zorn, B. Junno, T. Trepk, S. Bose, L. Samuelson, J.-T. Zettler, W. Richter, Phys. Rev. B 60 (1999) 11557.
[12] K.B. Ozanyan, P.J. Parbrook, M. Hopkinson, C.R. Whitehouse, Z. Sobiesierski, D.I. Westwood, J. Appl. Phys. 82 (1997) 474.
[13] M. Zorn, T. Trepk, J.-T. Zettler, B. Junno, C. Meyne, K. Knorr, T. Wethkamp, M. Klein, M. Miller, W. Richter, L. Samuelson, J. Appl. Phys. A 65 (1997) 333.
[14] D. Pahlke, J. Kinsky, C. Schultz, M. Pristovsek, M. Zorn, N. Esser, W. Richter, Phys. Rev. B 56 (1997) R1661.
[15] E.L. Briggs, D.J. Sullivan, J. Bernholc, Phys. Rev. B 54 (1996) 14362.
[16] W.G. Schmidt, E.L. Briggs, J. Bernholc, F. Bechstedt, Phys. Rev. B 59 (1999) 2234.
[17] F. Bechstedt, R. DelSole, G. Cappellini, L. Reining, Solid State Commun. 84 (1992) 765.
[18] J.E. Northrup, Phys. Rev. B 47 (1993) 10032.
[19] M. Rohlfing, P. Krüger, J. Pollmann, Phys. Rev. B 52 (1995) 1905.
[20] W.G. Schmidt, F. Bechstedt, Phys. Rev. B 55 (1997) 13051.
[21] M. Sauvage-Simkin, R. Pinchaux, J. Massies, P. Calverie, N. Jedrecy, J. Bonnet, I.K. Robinson, Phys. Rev. Lett. 62 (1989) 563.
[22] D.K. Biegelsen, R.D. Bringans, J.E. Northrup, L.E. Swartz, Phys. Rev. B 41 (1990) 5701.
[23] W.G. Schmidt, Appl. Phys. A 65 (1997) 581.
[24] S. Mirbt, N. Moll, A. Kley, J.D. Joannopoulos, Surf. Sci. 422 (1999) L177.
[25] N. Sanada, S. Mochizuki, S. Ichikawa, N. Utsumi, M. Shimomura, G. Kaneda, A. Takeuchi, Y. Suzuki, Y. Fukuda, S. Tanaka, M. Kamata, Surf. Sci. 419 (1999) 120.
[26] W.G. Schmidt, F. Bechstedt, Phys. Rev. B 54 (1996) 16742.
[27] W.G. Schmidt, N. Esser, A.M. Frisch, P. Vogt, J. Bernholc, F. Bechstedt, M. Zorn, Th. Hannappel, S. Visbeck, F. Willig, W. Richter, Phys. Rev. Lett. B 61 (2000) 16335.
[28] S. Albrecht, L. Reining, R. Del Sole, G. Onida, Phys. Rev. Lett. 80 (1998) 4510.
[29] S. Zollner, M. Garriga, J. Kirchner, J. Humlicek, M. Cardona, Phys. Rev. B 48 (1993) 7915.